World Applied Sciences Journal 33 (8): 1241-1257, 2015
ISSN 1818-4952

DOI: 10.5829/idosi.wasj.2015.33.08.15593

Behavior and Strength of Singly-Symmetric Continuous I-Beams

[1]A.H. Salem, [1]A.B. Abdelrahim and [2]R.H. Gabr

[1]Department of Structural Engineering, Ain Shams University, Cairo, Egypt
[2]Structural Engineer, Parsons International Limited,
Structural Engineering Department, Ain Shams University, Cairo, Egypt

Abstract: The design of singly-symmetric continuous I-beams did not take the same interest, in any standard or specification, as that of the doubly-symmetric simple I-beams. Thus, in this research, a numerical study using the finite element analysis was performed to study the elastic and inelastic behavior of singly-symmetric continuous I-beams bent about their major axis of bending. Nonlinear geometrical and material analyses were considered in this study. The finite element model was verified by comparing its results with experimental results of another research program. A parametric study was conducted to study the behavior and strength of continuous I-beams with two spans. Each span ranged from 3000 mm to 8000 mm and the web height ranged from 350 mm to 650 mm. Two cases of loading were considered in the study. In the first case, a concentrated load was applied at the middle of one of the two spans. In the second case, a concentrated load was applied at the middle of each span. The effect of loading position, with respect to the section height, on the behavior and strength of such beams was also investigated, as well as the effect of the mono-symmetric ratio. The ultimate moment capacities obtained from the finite element analysis were compared to those computed according to different standards and specifications. The comparison showed that the ultimate moment capacities computed according to the standards and specifications ranged from unconservative to conservative. Based on the conducted parametric study, an empirical design model was proposed for such beams.

Key words: Steel · Lateral-torsional · Buckling · Singly-symmetric · Continues I-beams · Ultimate moment capacity · Nonlinear · Finite element

INTRODUCTION

Open cross sections, such as singly-symmetric I-beams, bent about major axis, are widely used in many structural applications. The behavior of such beams does not take the same consideration as that of doubly-symmetric I-beams. At the present time the challenge to part of mono-symmetric theory still has not been fully resolved [1]. Elastic analysis was considered in the previously conducted research programs for continuous beams. For situations where there is no intermediate bracing within the span between the supports in the plane of loading, the influence of load position, with respect to the section height, should be considered [1]. This influence is not considered in most current standards and specifications. The elastic critical moment for bending in the plane of symmetry, M_{ocr}, is given in the SSRC Guide [2], for simply supported singly-symmetric I-beams, subjected to uniform moment, as follows:

$$M_{ocr} = \frac{\pi^2 EI_y}{L^2}\left[\frac{\beta_x}{2} + \sqrt{\left(\frac{\beta_x}{2}\right)^2 + \left(\frac{C_w}{I_y} + \frac{GJ}{EI_y}\frac{L^2}{\pi^2}\right)}\right] \quad (1)$$

where, E = elastic modulus; I_y = second moment of area about the minor axis; L = laterally unsupported length; C_w = warping constant; G = shear modulus; J = torsion constant; and β_x is approximated by Kitipornchai and Trahair [3], as follows:

$$\beta_x = 0.9h_o\left(\frac{2I_{yc}}{I_y} - 1\right)\left[1 - \left(\frac{I_y}{I_x}\right)^2\right] \quad (2)$$

Corresponding Author: A.B. Abdelrahim, Structural Engineering Department, Ain Shams University, Cairo, Egypt.

where, h_o = the distance between the centroid of the compression flange and that of the tension flange; I_{yc} = second moment of area of compression flange about minor axis; and I_x = second moment of area about the major axis.

Wang and Kitipornachai [4] studied singly-symmetric I-girders subjected to transverse loading applied at the shear center as well as the top and bottom flanges. They found that the value of the moment gradient coefficient, C_b, is extremely sensitive to the mono-symmetric ratio, ρ, when the load is applied at the shear center, where:

$$\rho = I_{yc} / I_y \quad (3)$$

Helwig *et al.* [5] investigated the lateral-torsional buckling of singly-symmetric I-beams, subjected to transverse loading consisting of either mid-span point load or uniformly distributed load applied at different depths, with respect to mid-depth of the cross section. For single-curvature bending, the finite element results showed that traditional coefficient, C_b, values can be used to estimate the critical moment of such beams. For reverse-curvature bending, the coefficient, C_b, was modified to correlate well with the finite element results. Mohsen *et al.* [6, 7, 8] investigated the behavior and capacity of overhanging singly-symmetric I-beams for various restraint conditions at the tip. Material and geometric nonlinearities were taken into consideration. A design model was introduced based on the results developed from the finite element analysis for such beams. Avik and Ashwini [9] studied the effect of distortional buckling of simply supported I-beams with different mono-symmetric ratios, ρ. Point and distributed loads were introduced, as well as top flange and bottom flange loading cases. Investigations revealed that moment modification factors, obtained from the study, agree with those of SSRC Guide [2], recommendations for fairly long beams because the buckling phenomenon is guided by flexural-torsional buckling. However, for short beams, the difference is significant since, C_b, values are dependent not only on the mono-symmetry ratio, ρ but also on the beam span to depth ratio, where the distortional buckling is predominant and hence, the flexural-torsional buckling solution gives overestimated critical loads. Avik and Ashwini [10] extended the investigation to the case of reverse-curvature bending where the buckling phenomenon becomes more complex than the case of single curvature bending because both of the flanges remain under compression at different locations along the beam length. Central point load and uniformly distributed load were presented. It was shown from the results that the available design specifications provide overestimated values of moment gradient coefficient, C_b. Trahair [11] presented the influence of restraints on the elastic buckling of monorails, without distortion, loaded at the bottom flange. In his study, Trahir used the finite element method to analyze simply supported, continuous, cantilever and overhanging beams with doubly-symmetric I-sections. Also, Trahair [12] studied the influence of the elastic lateral-distortional buckling of single span monorail I-beams on the strength of doubly-symmetric I-beams. He found that the distortion of a slender web lowers the elastic buckling resistance of an intermediate length beam below its flexural-torsional resistance. Yushi *et al.* [13] studied experimentally the effect of the adjacent non loaded span on the lateral-torsional buckling strength and deformation of the critical loaded span. Based on the study, the effective length concept, using the inflection points, was recommended for evaluating the ultimate strength of continuous beams. Salem *et al*. [14] studied the effect of loading position, with respect to section height, on the ultimate moment capacity of singly-symmetric continuous I-beams.

In this study, the nonlinear finite element analysis is used to investigate the behavior and strength of continuous singly-symmetric I-beams consisting of two spans. Concentrated loads at mid-spans are considered in the study. The effect of load position, with respect to the section height and the effect of mono-symmetric ratio, ρ, on the behavior and strength of such beams are studied. The effects of loaded and unloaded adjacent span as well as the effect of span length on the behavior and strength of such beams are also presented.

Finite Element Analysis and Verification: The multi-purpose finite element program ANSYS [15] is used to simulate the elastic and inelastic behavior of singly-symmetric continuous I-beams. All the nodes, elements, material properties, dimensions and boundary conditions are incorporated using shell elements. The element size is selected to maximize accuracy, while maintaining a reasonable computation time. Fig. 1 shows the used finite element mesh of such model and its coordinate system. The three supports of the beam are vertically restrained (Y-direction). One of the end supports (support 3), as shown in Fig. 2, is restrained in the longitudinal direction (Z-direction). The top flange is laterally restrained at the three supports (X-direction).

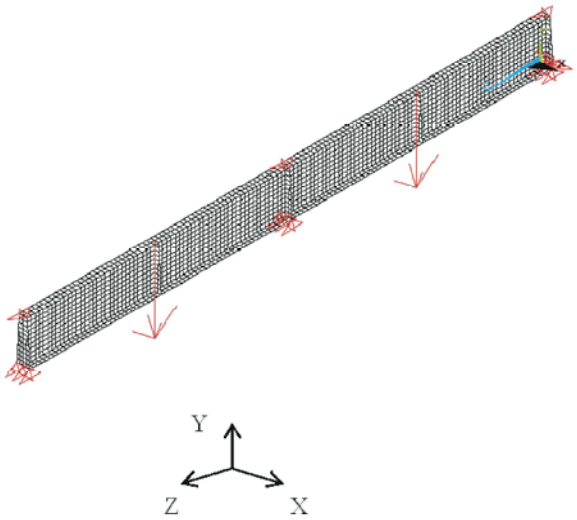

Fig. 1: Finite element model

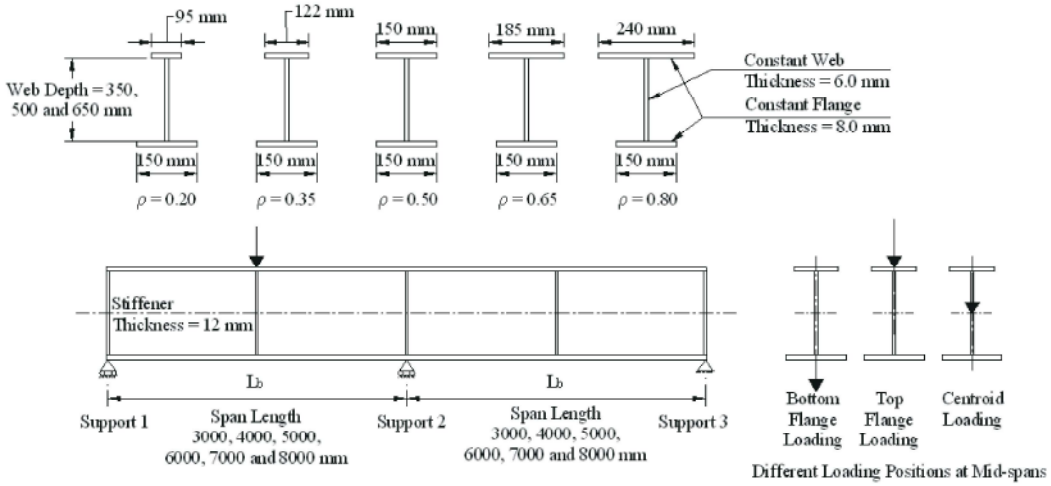

Fig. 2: Different parameters used in the parametric study

The in-plane and out-of-plane rotations are permitted (ROTZ and ROTY). These boundary conditions are applied to all specimens and the numerical models, as shown in Fig. 1. Stiffeners at loading and support locations are considered to eliminate any effect of local failure resulting from stress concentration over the loaded and supported nodes in the finite element model.

The concentrated load(s) are applied at the middle of the span length of the modeled beam. The applied concentrated load(s) are incrementally increased through successive load steps until failure occurred. Nonlinear finite element analysis is executed and both geometrical and material nonlinearities are considered. The Modified Newton-Raphson iteration technique is used to reach the conversion in each step. The initial imperfection is considered in the finite element model by incorporating out of straightness equal 1/1000 of the total length of the studied beams. Bilinear stress-strain response of material is incorporated in the analysis. The mechanical properties of the material used in the finite element model are summarized as follows: elastic modulus E = 210000 MPa, yield stress F_y = 280 MPa, Poisson's ratio, ν = 0.3 and tangent modulus = 0.01 of the used elastic modulus. The finite element model ability to depict the correct results to a reasonable degree of accuracy is investigated by checking the accuracy of the results obtained using the finite element model, in this study, versus the experimental work done by Mohsen *et al.* [6]. Table 1 presents the comparison between the results of the finite element analysis and those obtained experimentally. The ultimate loads obtained by the nonlinear finite element analysis are in good agreement with those obtained experimentally. The ultimate loads resulted from the finite element analysis are within a range of deviation

Table 1: Comparison between ultimate loads resulting from finite element analysis and those obtained experimentally by Mohsen *et al.* [6]

Specimen	P_u Experimental (kN)	P_u FEM (kN)	P_u FEM / P_u Exp.
OH-1	36.30	35.22	0.97
OH-2	30.02	30.49	1.02
OH-3	54.45	62.00	1.14
OH-4	46.70	47.09	1.01
OH-5	19.13	18.21	0.95
OH-6	10.10	11.38	1.13
Average	--	--	1.04

between +14% and -5% and an average of deviation of +4%, when compared to those obtained experimentally, which validates the finite element model.

Parametric Study: Once the validity of the finite element model is verified, a parametric study is conducted to study the effect of load position, with respect to the section height, on the ultimate moment capacity of the singly-symmetric continuous I-beams. The effects of mono-symmetric ratio, ρ, as well as the section height on the ultimate moment capacity of such beams are also investigated. As shown in Fig. 2, three different web heights are considered in the study; 350 mm, 500 mm and 650 mm, with a constant thickness of 6.0 mm for all cases giving web height to thickness ratio (h/w) of 58.33, 83.33 and 108.33, respectively. Six span lengths of the beam, L_b, are considered; 3000, 4000, 5000, 6000, 7000 and 8000 mm. Two different loading cases are considered in the study; single concentrated load at the mid-span over one span only and single concentrated load at the mid-span over each span of the two-span continuous beam. For each case of loading, three different load positions along the axis Y of the cross section are taken into account; load applied at the bottom flange, load applied at the top flange or load applied at the centroid of the section. Finally, five mono-symmetric ratios, ρ, are studied by fixing the bottom flange width to 150 mm and varying the top flange width to be 95 mm ($\rho = 0.20$), 122 mm ($\rho = 0.35$), 150 mm ($\rho = 0.50$), which is the doubly-symmetric cross-section case, 185 mm ($\rho = 0.65$) and 240 mm ($\rho = 0.80$). Both top and bottom flanges thicknesses are kept constant and equal 8.0 mm.

RESULTS AND DISCUSSION

The verified finite element model is adopted to investigate the behavior of the continuous singly-symmetric I-beams, with two spans, subjected to concentrated load(s). The results of the previously mentioned model are presented in the form of graphical relationships, representing the ultimate moment to plastic moment ratio (M_u/M_p) plotted against (L_b/r_t), where; L_b is the length between the supports (which are also the laterally- unsupported length of the top flange), as shown in Fig. 1, r_t, is the radius of gyration of the compression flange plus one-third of the web area in compression due to application of major axis bending alone. The plastic capacity of the section, M_p, of the I-beam is computed, as follows:

$$M_p = F_y \, x \, Z_x \tag{4}$$

where, F_y = specified minimum yield stress; and Z_x = plastic section modulus of the I-beam section.

For the case of single span loading (1P), the failure modes of the studied beams varied, depending on the span length and the mono-symmetric ratio. Failure by lateral-torsional buckling is observed for beams with mono-symmetric ratios, ρ, equal 0.20, 0.35 and 0.5 along all span lengths, as shown in Fig. 3. Beams with mono- symmetric ratios, ρ, equal 0.65 and 0.80, failed by flange yielding for short spans, while failure due to combination of flange yielding and lateral-torsional buckling is observed for beams with longer spans, as shown in Fig. 4. For the case of double span loading (2P), the failure modes of the studied beams are close to those of single span loading case, as shown in Fig. 5.

Figures 6 to 35 show that for all the studied cross-sections, the ultimate moment capacity to the plastic moment ratio (M_u/M_p) decreased with increasing the lateral-torsional slenderness ratio (L_b/r_t). This applies to all load positions and load cases as well as all mono-symmetric ratios. The rate, at which the ultimate moment capacity is reduced, increases as the mono-symmetry ratio, ρ, increases. This is due to the weakness of the cross-sectional properties for beams with low values of mono-symmetric ratio, ρ, which forces the beam to fail by lateral-torsion buckling. Meanwhile, for beams with high values of mono-symmetric ratio, ρ, the plastic limit capacity could be reached.

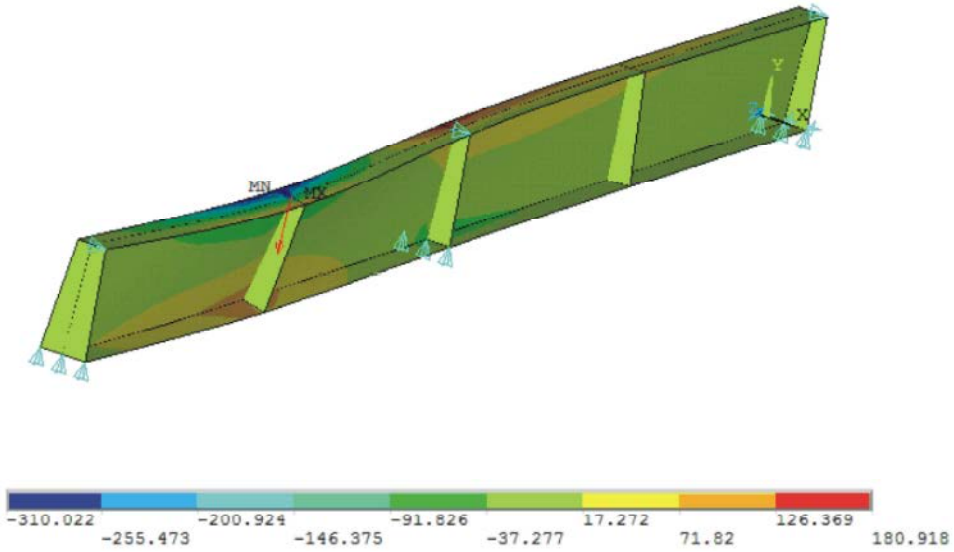

Fig. 3: Failure by lateral-torsional buckling for beams with single loading case (1P)

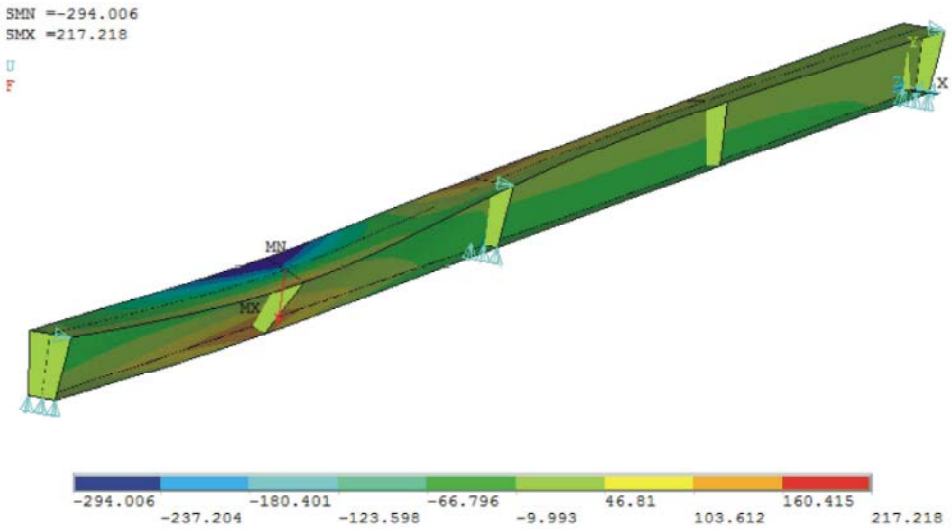

Fig.4: Failure by combined yielding and lateral-torsional buckling for beams with single loading case (1P)

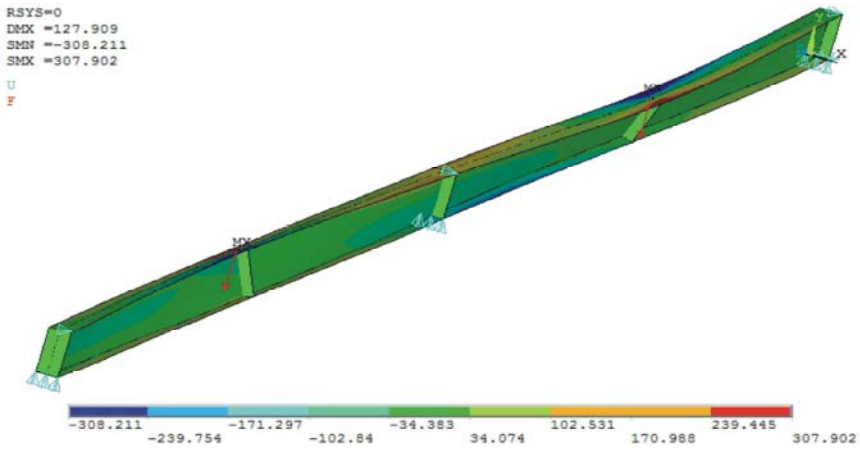

Fig. 5: Failure by lateral-torsional buckling for beams with double loading case (2P)

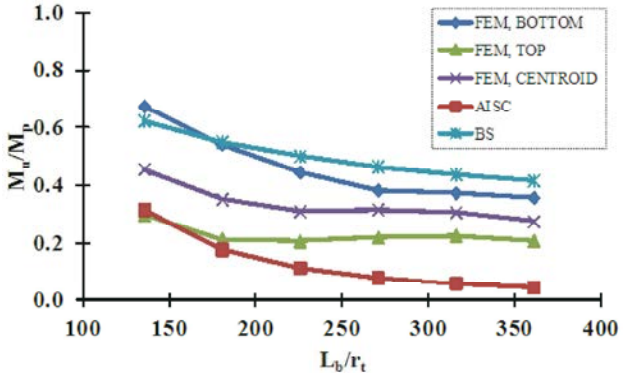

Fig. 6: Ultimate moment capacity for single loading case, web height 350 mm and ρ = 0.20

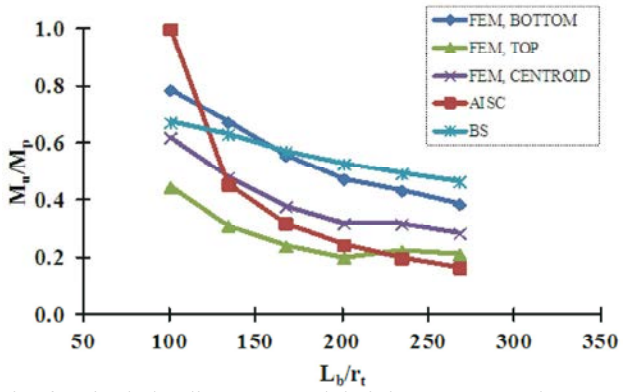

Fig. 7: Ultimate moment capacity for single loading case, web height 350 mm and ρ = 0.35

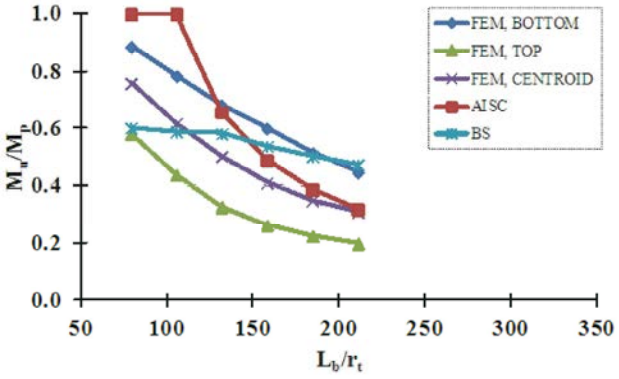

Fig. 8: Ultimate moment capacity for single loading case, web height 350 mm and ρ = 0.50

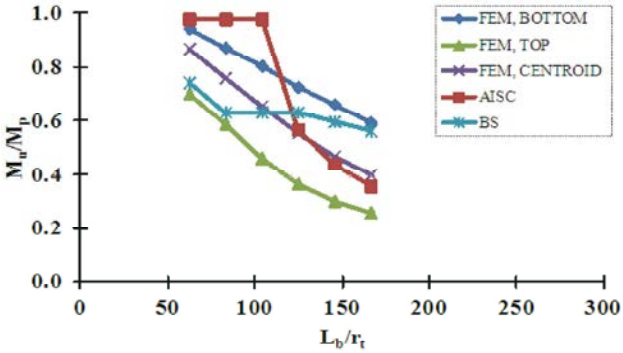

Fig. 9: Ultimate moment capacity for single loading case, web height 350 mm and ρ = 0.65

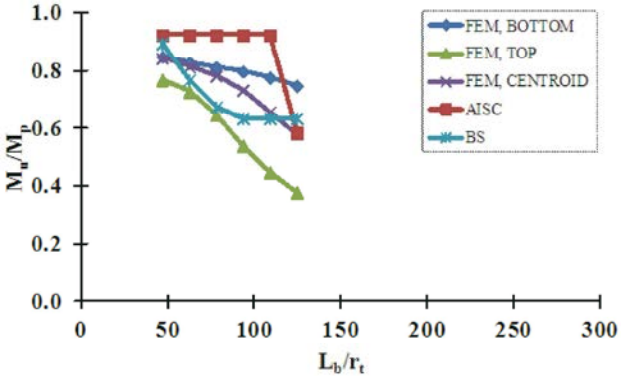

Fig. 10: Ultimate moment capacity for single loading case, web height 350 mm and ρ = 0.80

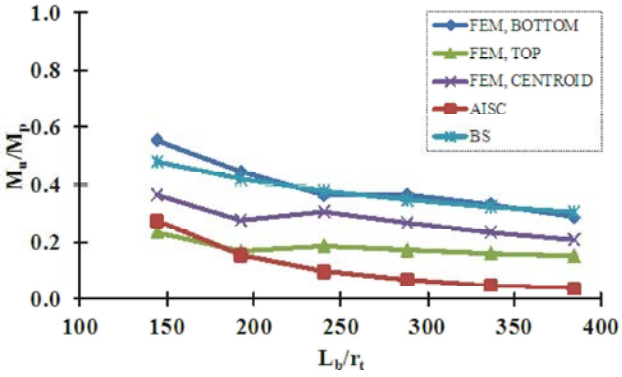

Fig. 11: Ultimate moment capacity for single loading case, web height 500 mm and ρ = 0.20

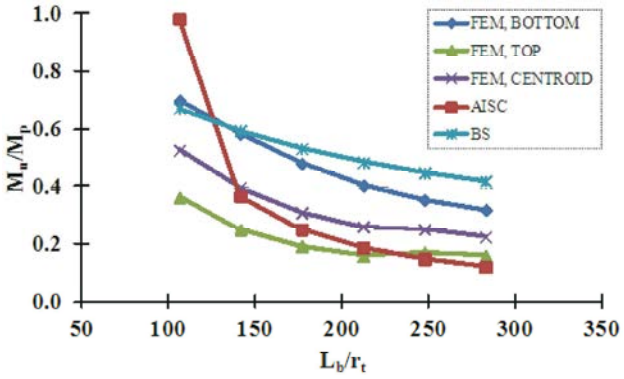

Fig. 12: Ultimate moment capacity for single loading case, web height 500 mm and ρ = 0.35

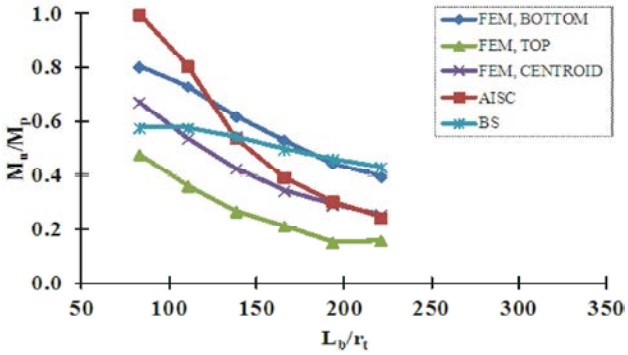

Fig. 13: Ultimate moment capacity for single loading case, web height 500 mm and ρ = 0.50

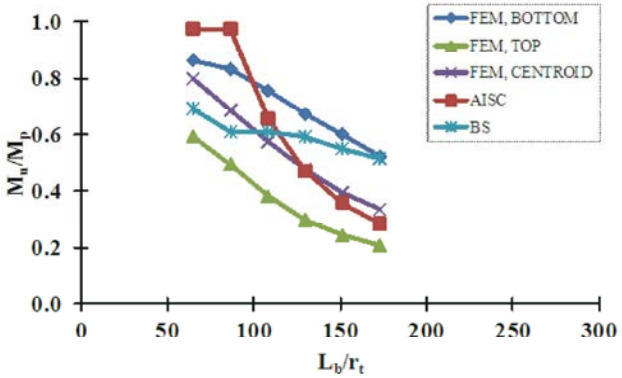

Fig. 14: Ultimate moment capacity for single loading case, web height 500 mm and ρ = 0.65

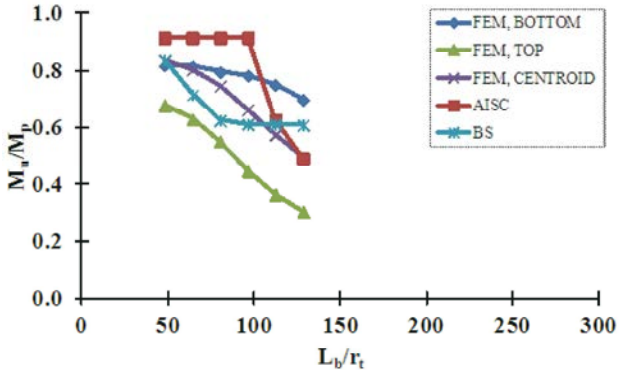

Fig. 15: Ultimate moment capacity for single loading case, web height 500 mm and ρ = 0.80

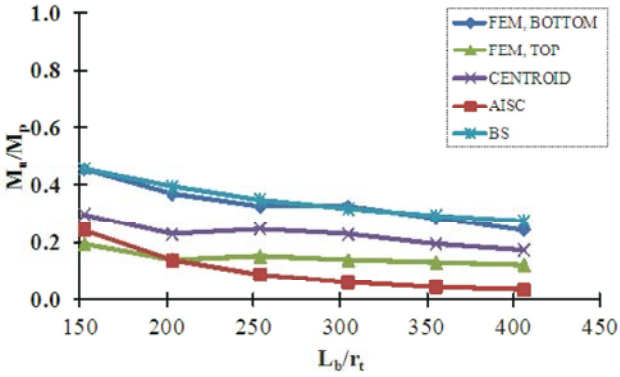

Fig. 16: Ultimate moment capacity for single loading case, web height 650 mm and ρ = 0.20

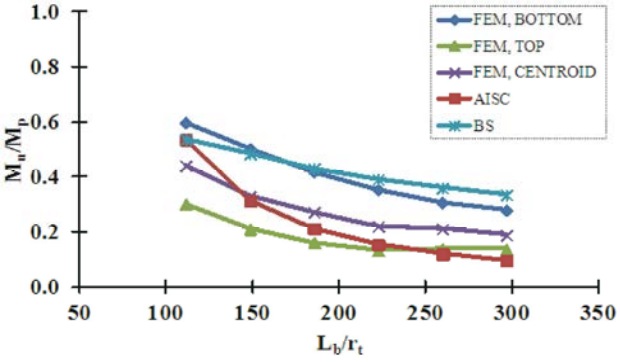

Fig. 17: Ultimate moment capacity for single loading case, web height 650 mm and ρ = 0.35

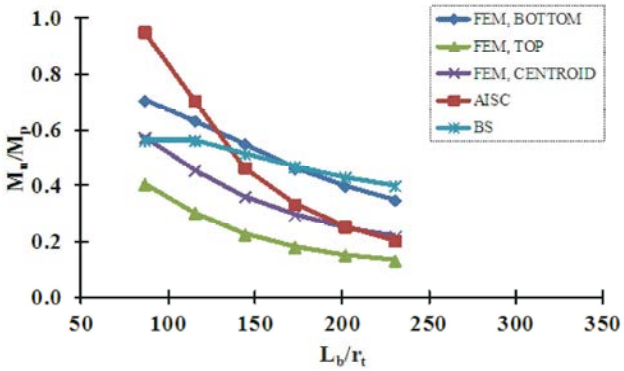

Fig. 18: Ultimate moment capacity for single loading case, web height 650 mm and ρ = 0.50

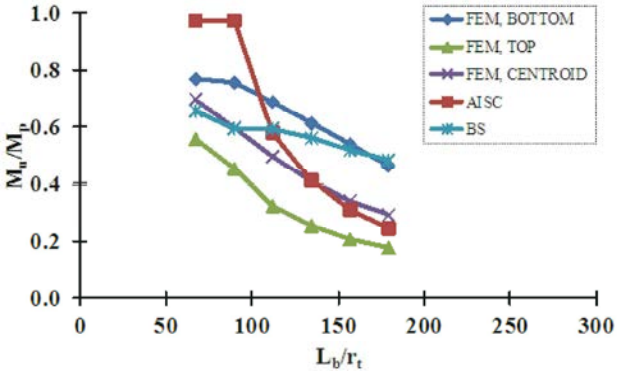

Fig. 19: Ultimate moment capacity for single loading case, web height 650 mm and ρ = 0.65

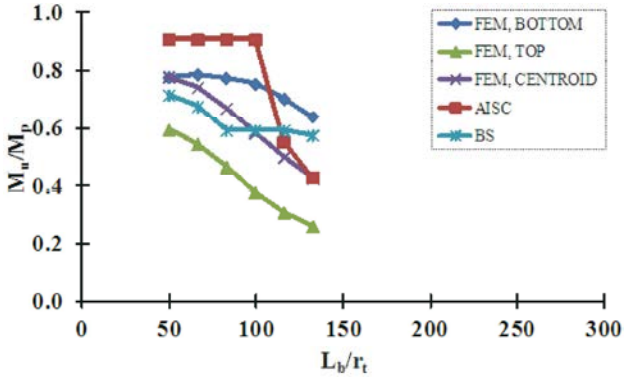

Fig. 20: Ultimate moment capacity for single loading case, web height 650 mm and ρ = 0.80

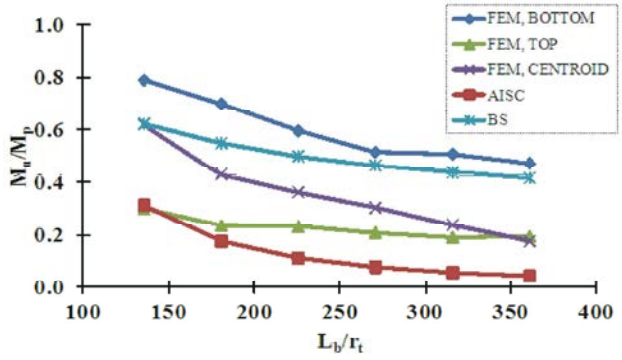

Fig. 21: Ultimate moment capacity for double loading case, web height 350 mm and ρ = 0.20

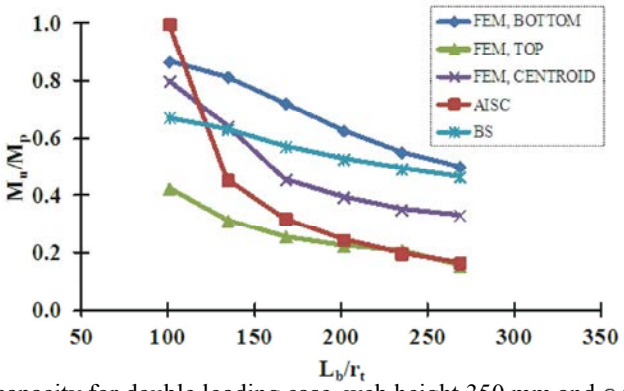

Fig. 22: Ultimate moment capacity for double loading case, web height 350 mm and ρ = 0.35

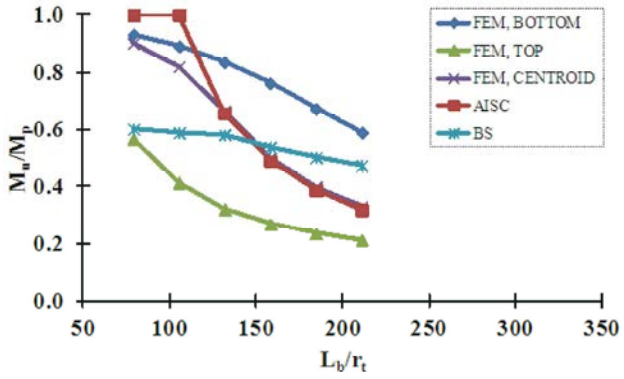

Fig. 23: Ultimate moment capacity for double loading case, web height 350 mm and ρ = 0.50

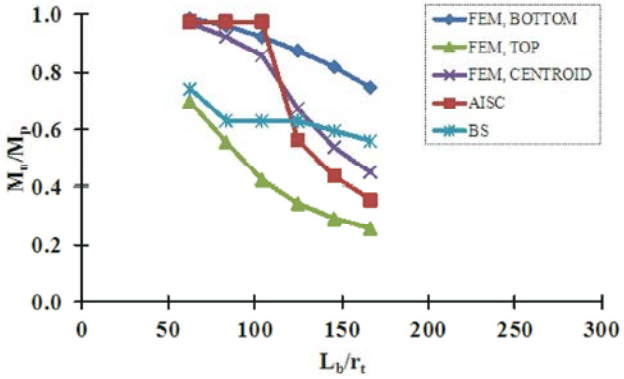

Fig. 24: Ultimate moment capacity for double loading case, web height 350 mm and ρ = 0.65

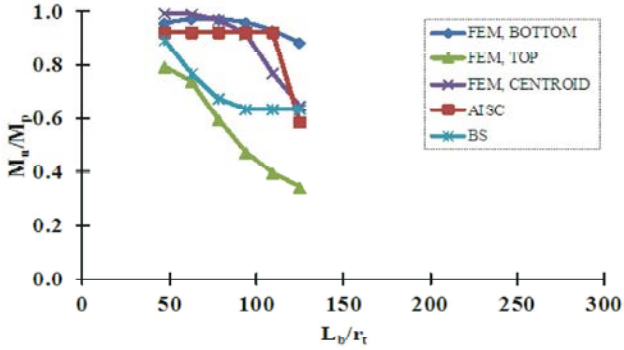

Fig. 25: Ultimate moment capacity for double loading case, web height 350 mm and ρ = 0.80.

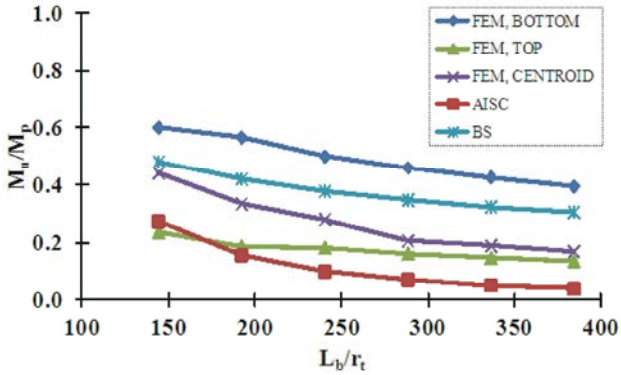

Fig. 26: Ultimate moment capacity for double loading case, web height 500 mm and ρ = 0.20

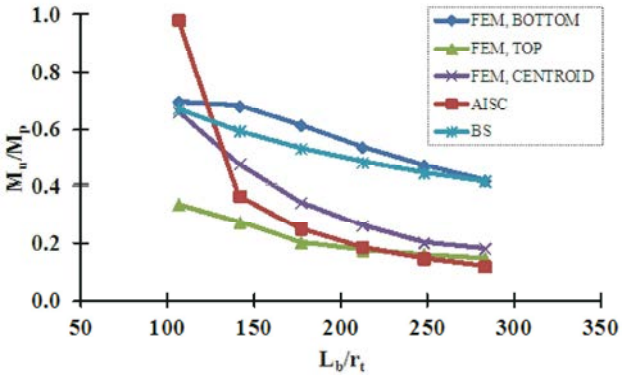

Fig. 27: Ultimate moment capacity for double loading case, web height 500 mm and ρ = 0.35

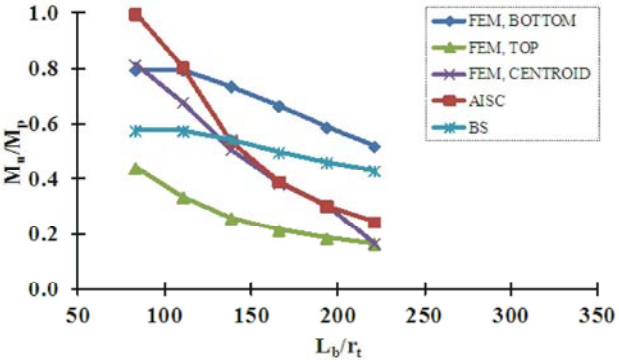

Fig. 28: Ultimate moment capacity for double loading case, web height 500 mm and ρ = 0.50

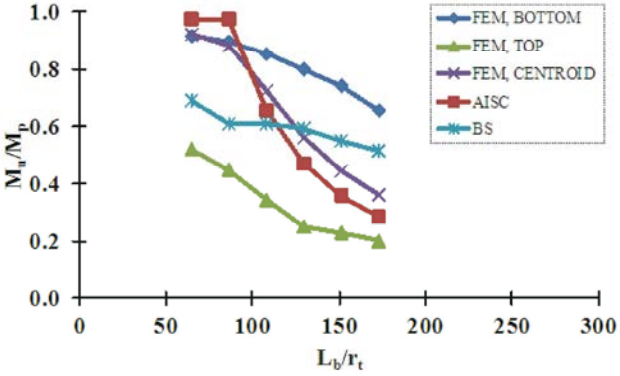

Fig. 29: Ultimate moment capacity for double loading case, web height 500 mm and ρ = 0.65

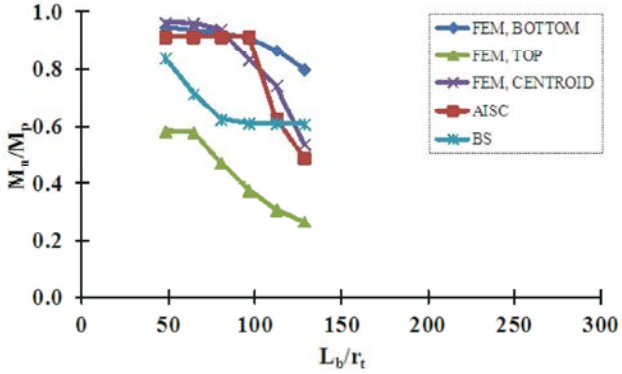

Fig. 30: Ultimate moment capacity for double loading case, web height 500 mm and ρ = 0.80

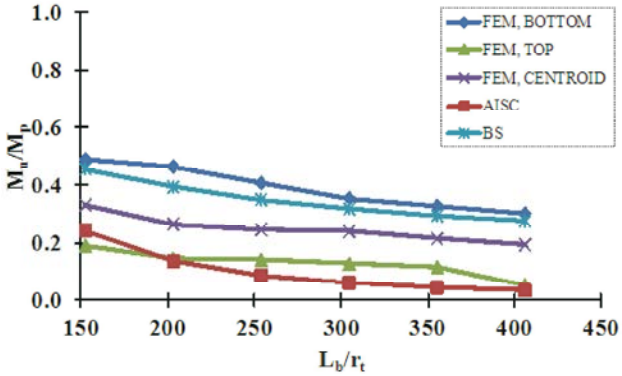

Fig. 31: Ultimate moment capacity for double loading case, web height 650 mm and ρ = 0.20

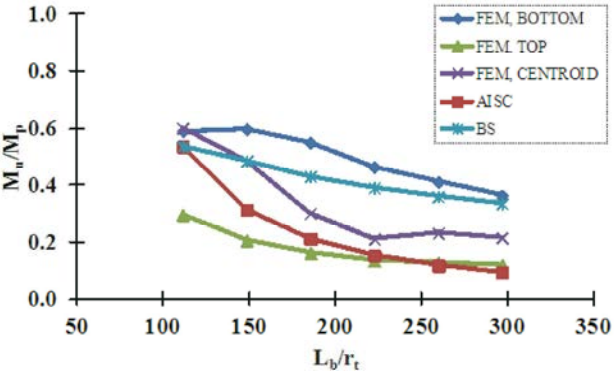

Fig. 32: Ultimate moment capacity for double loading case, web height 650 mm and ρ = 0.35

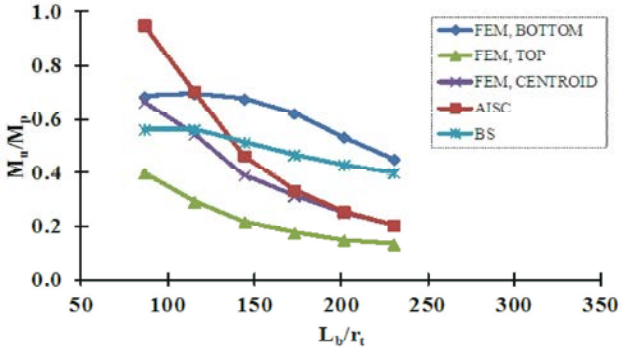

Fig. 33: Ultimate moment capacity for double loading case, web height 650 mm and ρ = 0.50

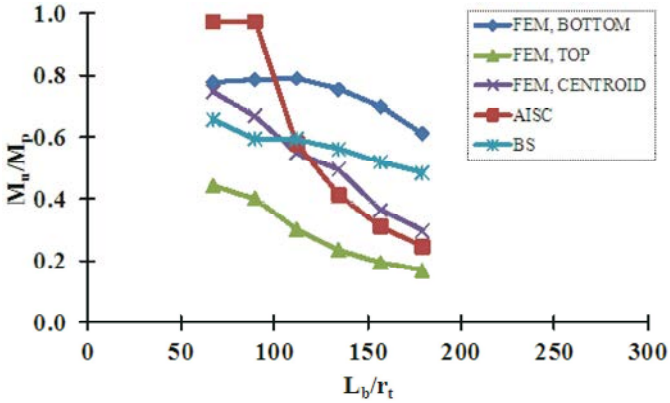

Fig. 34: Ultimate moment capacity for double loading case, web height 650 mm and ρ = 0.65

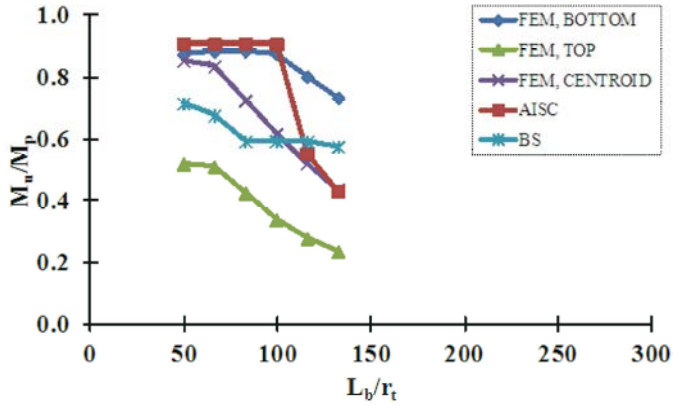

Fig. 35: Ultimate moment capacity for double loading case, web height 650 mm and ρ = 0.80

The figures also show that the lowest values of ultimate moment capacities are obtained when the loads are applied at the top flange. On the other hand, the highest values of ultimate moment capacities are obtained when the loads are applied at the bottom flange. The main reason for this behavior is due to the fact that the section of such beams, when loaded at top flange, tends to destabilize the section increasing the chance for early failure by lateral-torsional bucking, while it is more likely to keep the section of such beams stable against lateral-torsional buckling, when loaded at the bottom flange. For beams with mono-symmetric ratios, ρ, equal 0.20 and 0.35, the difference between the ultimate moment capacities, obtained from top flange loading and those obtained from bottom flange loading could reach 40%, for both cases of loading (1P and 2P). This difference is also observed for beams with mono-symmetry ratios, ρ, equal 0.50, 0.65 and 0.80, only for higher values of (L_b/r_t) for all web heights and both cases of loading (1P and 2P). In addition, the same difference is observed for beams with mono-symmetric ratios, ρ, equal 0.50, 0.65 and 0.80 and low values of (L_b/r_t), when the web heights equal 350 mm and 500 mm and single span loading case (1P), as shown in Figures 8 to 10 and Figures 13 to 14. For beams with web heights equal 650 mm and loaded at single span only (1P), the difference between the ultimate moment capacities of beams with top flange loading and those of beams with bottom flange loading, increases gradually to 60%, when the mono-symmetric ratio, ρ, equal 0.50 and when low values of (L_b/r_t) is considered. This difference jumps to 80% for beams with mono-symmetric ratios, ρ, equal 0.65 and 0.80, when the web height equal 650 mm and low values of (L_b/r_t) are considered.

For the studied cases of loading (1P and 2P), the beams with mono-symmetric ratios, ρ, equal 0.20 and 0.35, the ultimate moment to the plastic moment ratio (M_u/M_p) stays low between 0.10 and 0.40 for top flange loading and between 0.40 and 0.70 for bottom flange loading. This is due to the lateral-torsional buckling failure mode. For beams with mono-symmetric ratios, ρ, equal 0.50, 0.65 and 0.80, the ultimate moment to the plastic moment ratio (M_u/M_p) is noticed to be between 0.20 and 0.75 for top flange loading and between 0.65 and 0.95 for bottom flange loading. This is due to the yielding of the sections,

especially, at low values of (L_b/r_t). For the case of double span loading (2P), the ultimate moment capacities of beams with mono-symmetric ratios, ρ, equal 0.35, 0.50, 0.65 and 0.80 and loaded at bottom flange, are close to those of beams loaded through the section centroid, especially, when low values of (L_b/r_t) are considered, for all web heights. For the same beams, loaded at the section centroid, as (L_b/r_t) increases, the ultimate moment capacity decreases gradually and becomes much closer to those of beams loaded at top flange. This could be explained by that the beams tend to fail by yielding, especially, when low values of (L_b/r_t) are considered. However, as (L_b/r_t) increases, the beams tend to fail by lateral-torsional buckling.

For the case of single span loading (1P), beams with mono-symmetric ratio, ρ, equal 0.80 and loaded through the centroid, as shown in Figures 10, 15 and 20, the ultimate moment capacities are close to those of such beams, loaded at bottom flange, when (L_b/r_t) values ranged from 40 to 130, for all studied web heights. The effect of adjacent loaded span is more significant on the ultimate moment capacity of beams, which are loaded at the bottom flange. The ultimate moment capacity of such beams is higher than those of singly loaded beams by a range of 20%. This range is reduced to 15%, when the beams loaded at the top flange or through the section centroid.

Current Standards and Specifications: In this section, the ultimate moment capacities resulting from the finite element analysis are compared to those computed according to the AISC Specification [16] and the BS5950:1 [17], as follows:

Case of Single Span Loading (1P): Figures 6 to 20 show that the ultimate moment capacities, computed according to the AISC Specification [16], present the most conservative results for beams with mono-symmetric ratio, ρ, equal 0.20, due to lateral-torsional buckling failure mode, whereas the ultimate moment capacities, computed according to the BS5950:1 [17], present the least conservative results and show a reasonable agreement with those obtained from the finite element, when the beam is loaded at bottom flange. As the mono-symmetric ratio, ρ, increases, the ultimate moment capacities, computed according to the AISC Specification [16], change from being the most conservative for beams with mono-symmetric ratio, ρ, equal 0.20, to the least conservative for beams with mono-symmetric, ρ, equal 0.80, where the failure mode of the beams takes place at the plastic stage of the section. The figures also show that the ultimate moment capacities of such beams, computed according to the BS5950:1 [17], are close to those resulting from the finite element analysis when the beams, loaded at bottom flange. Meanwhile, for beams with mono-symmetric ratios, ρ, equal 0.50 and 0.65, the comparison between the ultimate moment capacities, computed according to the AISC Specification [16] and those computed according to the BS5950:1 [17] depends mainly on the (L_b/r_t) ratio. The ultimate moment capacities computed according to the AISC Specification [16] show higher values than those computed according to the BS5950:1 [17] for beams with spans equals to 3000, 4000 and 5000 mm and lower than those computed according to the BS5950:1 [17] for beams with spans equal 5 to 6000, 7000 and 8000 mm.

Case of Double Span Loading (2P): Figures 21 to 35 show that the ultimate moment capacities, computed according to the AISC Specification [16], change from being the most conservative for beams with mono-symmetric ratio, ρ, equal 0.20 to the least conservative for beams with mono-symmetric ratio, ρ, equal 0.80. The ultimate moment capacities, computed according to the AISC Specification [16] and the BS5950:1 [17] for this case of loading, are close to those of single span loading case, as the failure is located at the mid span section for both cases of loading. In this case of loading, the ultimate moment capacities, computed according to the BS5950:1 [17] are not close to those obtained from the finite element analysis, for the beams loaded at the bottom flange, but they are between those of beams loaded at bottom flange and those of beams loaded at top flange, unlike those of the single span loading case.

Proposed Design Model: Based on the parametric study results, an empirical design model of such beams is developed and proposed, as follows:

$$\frac{M_u}{M_p} = a + b\frac{L_b}{r_t} + c\left(\frac{L_b}{r_t}\right)^2 + d(\rho) + e(\rho)^2 \quad (5)$$

where, M_u = ultimate moment capacity of the singly-symmetric continuous I-beam; M_p = plastic moment, as per equation (4); L_b = distance between lateral supports; r_t = radius of gyration of the compression flange plus one-third of the web area in compression; ρ = mono-symmetric ratio, which is calculated as the ratio of the moment of inertia about the minor axis of the compression flange to the moment of inertia about the minor axis of the whole cross section; and (a), (b), (c), (d) and (e) = coefficients given in Table 2.

Table 2: Proposed model coefficients

Section Classification	Load case	Load position	L_b/r_t	a	b	C	d	e
Compact sections	Single load over one span (1P)	Bottom flange	40-130	0.738	2.18E-03	-2.25E-05	0.254	-2.59E-01
			130-360	1.352	-5.95E-03	9.28E-06	-0.192	1.10E-01
		Top flange	40-130	0.912	-4.90E-03	-6.80E-07	0.077	-3.17E-02
			130-360	0.665	-3.75E-03	7.20E-06	0.082	-1.73E-01
		Centroid	40-130	0.859	-9.40E-04	-1.80E-05	0.105	-3.08E-02
			130-360	0.999	-5.13E-03	9.09E-06	0.006	-9.61E-02
	Single load over two spans (2P)	Bottom flange	40-130	0.900	1.97E-03	-1.82E-05	-0.274	3.18E-01
			130-360	1.443	-5.63E-03	8.30E-06	-0.045	-6.52E-02
		Top flange	40-130	1.012	-5.36E-03	4.12E-06	-0.312	2.00E-01
			130-360	0.584	-2.54E-03	4.11E-06	0.009	-1.56E-01
		Centroid	40-130	0.826	6.55E-03	-6.23E-05	-0.252	2.34E-01
			130-360	1.358	-6.81E-03	1.01E-05	0.146	-5.01E-01
Noncompact sections	Single load over one span (1P)	Bottom flange	80-200	1.052	-5.20E-03	8.78E-06	0.290	-3.65E-01
			200-400	0.598	-5.65E-04	-1.48E-07	-0.585	7.94E-01
		Top flange	80-200	0.878	-7.43E-03	1.83E-05	0.256	-3.59E-01
			200-400	0.111	5.43E-04	-1.16E-06	-0.058	-5.35E-03
		Centroid	80-200	1.105	-8.63E-03	2.06E-05	0.394	-5.17E-01
			200-400	0.337	1.63E-04	-9.59E-07	-0.408	4.54E-01
	Single load over two spans (2P)	Bottom flange	80-200	0.548	6.16E-04	-5.00E-06	0.283	-3.36E-02
			200-400	0.898	-2.36E-03	2.36E-06	-0.042	6.92E-02
		Top Flange	80-200	0.909	-7.89E-03	2.07E-05	0.180	-3.01E-01
			200-400	0.036	1.24E-03	-2.63E-06	-0.130	9.78E-02
		Centroid	80-200	1.045	-6.67E-03	8.90E-06	1.235	-1.85E+00
			200-400	0.545	-1.33E-03	1.43E-06	-0.317	2.46E-01

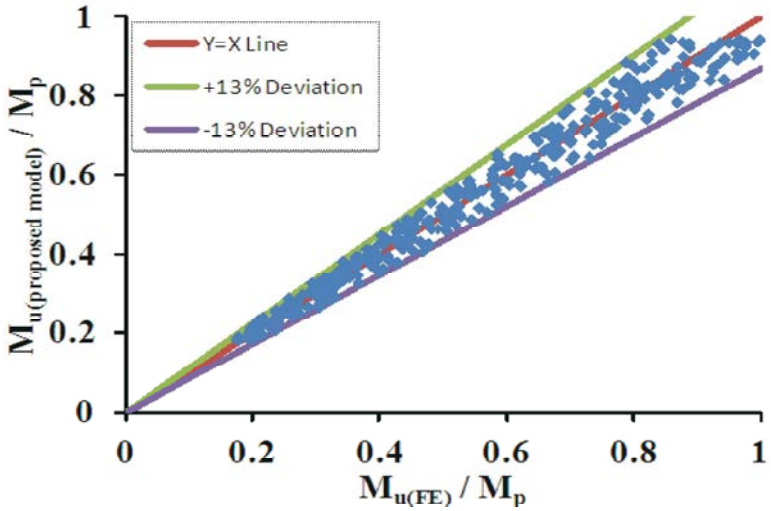

Fig. 36: Comparison between (M_u/M_p) ratio computed according to the proposed model and those obtained from the finite element analysis for compact sections

As shown in Table 2, selecting the coefficients depends on the section class, either compact or noncompact. The classification limit is based on that presented in Table (B4.1) of the AISC Specification [16]. The coefficients selection also depends on the loading case (1P or 2P) and (L_b/r_t) ratio as well as the loading position, with respect to the section height. The accuracy of the proposed design model is verified by comparing its results with those obtained through the finite element analysis.

Figures 36 and 37 show that the ultimate moment capacities, computed according to the proposed design model are in the range of ±13% of those resulting from the finite element analysis. Figure 36 shows the comparison for the beams with compact sections, while Fig. 37 shows the comparison for the beams with noncompact sections.

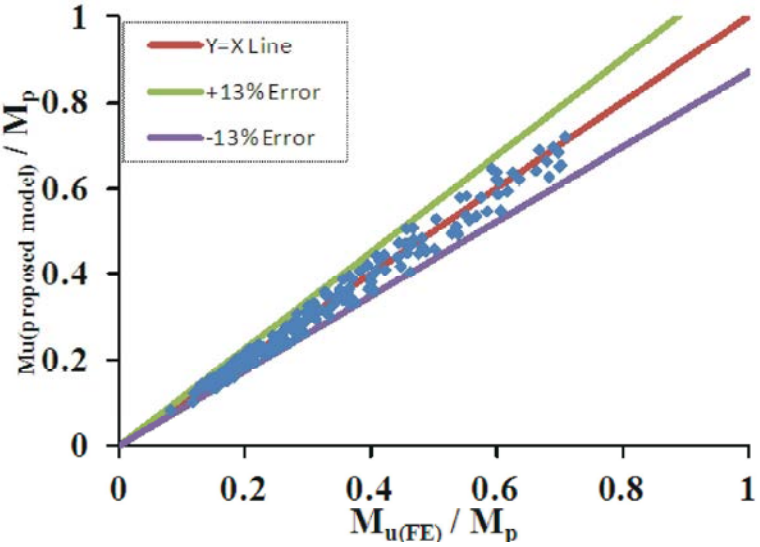

Fig. 37: Comparison between (M_u/M_p) ratio computed according to the proposed model and those obtained from the finite element analysis for noncompact sections

SUMMARY AND CONCLUSIONS

Due to the lack of research of singly-symmetric continuous I-beams, an extensive research program has been conducted to investigate the behavior of such beams. A finite element model, correlated well with the experimental results of another research program, was developed using the ANSYS finite element program [15] to simulate the behavior of singly-symmetric continuous I-beams. The lateral-torsional buckling behavior and yielding of the cross section were taken into account. Nonlinear material and geometrical analyses were performed. Once the validity of this model was verified, an extensive parametric study was conducted. Continuous beams with two equal-spans were investigated in this study. Each span ranged from 3000 mm to 8000 mm. The web height ranged from 350 mm to 650 mm. The top flanges of the beams were laterally restrained at the vertical support sections. Two different loading cases were considered in the study; single concentrated load at the mid-span over one span only and single concentrated load at the mid-span over each span of the two-span continuous beam. For each case of loading, three different load positions, with respect to the section height, were taken into account; load applied at bottom flange, load applied at top flange and load applied at the centroid of the section. Finally, five mono-symmetric ratios, ranged from 0.2 to 0.8, were incorporated in the study.

Most of the studied beams with low mono-symmetric ratios, failed by lateral-torsional buckling, while those with high mono-symmetric ratios, failed by flange yielding (especially, for beams with short spans) or by interaction between flange yielding and lateral-torsional buckling (especially, for beams with long spans). The ultimate moment capacities, computed according to the current standards and specifications varied from conservative to unconservative when compared to those obtained from the finite element analysis. An empirical design model, based on the results developed from the parametric study, was proposed. The ultimate moment capacities, computed according to the proposed design model, were compared to those obtained from the finite element analysis. The comparison showed that the proposed design model results had a strong correlation with those of the finite element analysis.

REFERENCES

1. Ziemian, R.D., 2010. Guide to Stability Design Criteria for Metal Structures, 6th Edition, Structural Stability Research Council. John Wiley & Sons Inc, Hoboken (NJ).
2. Galambos, T.V., 1998. Guide to Stability Design Criteria for Metal Structures, 5th Edition, Structural Stability Research Council. John Wiley & Sons, New York.
3. Kitipornchhai, S. and N.S. Trahair, 1980. Buckling properties of monosymmetric I-beams. ASCE J. Struct. Div., 106(ST5): 941-958.
4. Wang, C.M. and S. Kitipornchai, 1986. Buckling capacities of monosymmetric I-beams. Journal of Structural Engineering, ASCE, 112(11): 2373-2391.

5. Helwig, T.A., K.H. Frank and J.A. Yura, 1997. Lateral-torsional buckling of singly symmetric I-beams. Journal of Structural Engineering, ASCE, 123(9): 1172-1179.
6. Mohsen, H.A., A.M. Fadel, A.B. Abdel-Rahim and B.L. Gindi, 2007. Experimental study of mono-symmetric over-hanging I-beams steel sections. HBRC International Journal, 3(2): 55-66.
7. Mohsen, H.A., A.M. Fadel, A.B. Abdel-Rahim and B.L. Gindi, 2007. Proposed design model for mono-symmetric over-hanging I-beams (Part I-Laterally restrained). The 12th International Colloquium on Structural & Geotechnical Engineering, December 10-12, Ain Shams University, Cairo, Egypt.
8. Mohsen, H.A., A.M. Fadel, A.B. Abdel-Rahim and B.L. Gindi, 2007. Proposed design model for mono-symmetric over-hanging I-beams (Part II-Laterally unrestrained). The 12th International Colloquium on Structural & Geotechnical Engineering, December 10-12, Ain Shams University, Cairo, Egypt.
9. Avik, S. and K. Ashwini, 2006. Distortional buckling in monosymmetric I-beams. Thin-Walled Structures, 44: 51-56.
10. Avik, S. and K. Ashwini, 2006. Distortional buckling in monosymmetric I-beams: Reverse-curvature bending. Thin-Walled Structures, 44: 721-725.
11. Trahair, N.S., 2008. Lateral buckling of monorails. Engineering Structures, Elsevier, 30: 3213-3218.
12. Trahair, N.S., 2009. Lateral-distortional buckling of monorails. Engineering Structures, Elsevier, 31: 2873-2879.
13. Yushi, F., I. Yoshito and H. Ryoji, 1982. Lateral buckling tests on welded continuous beam. Journal of Structural Engineering. ASCE, 106(ST10): 2245-2263.
14. Salem, A.H., A.B. Abdelrahim and R.H. Gabr, 2014. Effect of load position on the ultimate moment capacity of singly-symmetric continuous I-beams. Civil Engineering Research Magazine, CERM, 36(1): 202-228.
15. ANSYS, 2009. Finite element program (Swanson Analysis System, Inc., Release 12.0.1), (ANSYS Inc).
16. American Institute of Steel Construction, Specification for Structural Steel Buildings, 2010.
17. BS5950: Part1:2000. British Standard Part1 Code of Practice for Design in Simple and Continuous Construction: Hot Rolled Section.